Hindawi
Advances in Materials Science and Engineering
Volume 2020, Article ID 9048508, 8 pages
https://doi.org/10.1155/2020/9048508

Research Article

A Fatigue Life Prediction Method for the Drive System of Wind Turbine Using Internet of Things

Hang Zhou, Shi-Jun Yi, Ya-Fei Liu, Yong-Quan Hu, and Yong Xiang

School of Computer Engineering, Chengdu Technological University, Chengdu 611731, China

Correspondence should be addressed to Yong Xiang; zhouchcdsc@163.com

Received 24 June 2020; Revised 4 August 2020; Accepted 6 August 2020; Published 27 August 2020

Guest Editor: Shun-Peng Zhu

The wind turbine drive system is one of the key components in converting wind energy into electrical energy. The life prediction of drive system is very important for the maintenance of wind turbine. With increasing capacity, the wind turbine system has become more complicated. Consequently, for the life prediction of drive system, it is necessary to consider the problems of multi-information fusion of big data, quantification of time-varying dynamic loads, and analysis of multiple-damage coupling. In order to solve the above challenges, the fatigue life analysis and evaluation method considering the interaction of coupled multiple damages are proposed in this study. The hierarchical Bayesian theory with fault physics technology is introduced to deal with the uncertainty of wind turbine drive system. Then, a time-varying performance analysis model is established based on the multiple-damage coupling competition failure mechanism. Moreover, the Internet of Things (IoT) technology is introduced and combined with the proposed model. Through the data collection by IoT, the time-stress curve of drive system can be obtained. A case study about the remaining fatigue life estimation of drive system is utilized to illustrate the effectiveness of the proposed method.

1. Introduction

Wind energy is a common clean and renewable energy. The effective utilization of wind energy can reduce the energy crisis and protect the environment. The early development of wind energy is mainly carried out on land. Engineers have successfully built many onshore wind turbines. Compared with offshore wind farms, onshore wind farms are more mature in technology and management [1]. Generally, the offshore wind farms are located on the ocean and have very little impact on humans. Therefore, offshore wind power will account for more proportion in the future wind power industry.

Uncertain environment has restricted the development of offshore wind turbines and threatened the wind turbine drive system security [2]. The design requirements for offshore wind farms are more difficult than those for onshore wind farms [3–6]. Risk assessment can improve the reliability of systems [7–11]. For wind turbine drive system, it is important to study the failure mechanism, fault diagnosis, and life prediction of key components. Accordingly, recent research involves multiple subjects like dynamics, material mechanics, fatigue, reliability, and signal analysis [12, 13].

Taking the wind turbine planetary gearbox as an example, the dynamic analysis mainly focuses on the characteristics of gears and bearings. The gear dynamics model mainly analyzes the gear mesh stiffness characteristics [14], the tooth surface contact force [15, 16], and the influence of assembly and machining errors [17]. The bearing dynamics model mainly analyzes the interaction force between the rolling element and the cage [18, 19] and the influence of the cage parameters on the bearing characteristics [20]. During the operation of the gearbox, the tooth surfaces and roots are subjected to alternating and impact loads, which leads to fatigue damage of the gears. Many uncertainties also cause the failure of the bearing. Thus, the dynamic model is proposed for failure mechanism analysis, fault diagnosis, and life prediction.

The research of gear failure mechanism starts from the tooth root crack [21], the tooth surface pitting [15], and the relationship between crack change and meshing stiffness change [14]. The research of bearing failure mechanism

starts from the change of bearing rolling element clearance [22, 23], the number of pressure rolling elements [24], the lubrication characteristics [25] and the cage flexibility characteristics [26]. Recent research results include rolling bearing-rotor systems [27], gear transmission systems [28], gear-rotor-bearing system [29], and gearbox bearing system [30].

The main working mode of wind turbine planetary gearbox is that the load changes with the wind speed. Therefore, the fault diagnosis is the core technology in research process. Many methods have been proposed, such as using instantaneous power spectrum and genetic programming methods to identify fault feature parameters [31]; fault diagnosis of rotating machinery under variable operating conditions based on wavelet packet coefficients and entropy information indicators [32]; and fault information extraction based on the Vold–Kalman method [33].

In the process of fault diagnosis, it is necessary to analyze the internal and external load characteristics. However, the current research mainly focuses on the relationship between a certain fault state and system dynamics. These research works are short on developing dynamic fault response mechanism. This paper proposes the coupling fault diagnosis mechanism and the fatigue life prediction method based on wind farm complex conditions.

Many scholars have carried out research on product remaining life prediction methods, such as model-based methods, data-driven methods, and hybrid methods [34–37]. The product monitoring data have the characteristics of large quantity and variety. Consequently, it is necessary to achieve automatic real-time analysis of product monitoring data by the Internet of Things (IoT). Deep learning methods are also effective ways to solve this problem. However, most of them cannot solve the product remaining life prediction problems. Hence, the product remaining life prediction based on the Internet of Things has a good research prospect.

In this paper, a remaining life prediction method based on deep learning is proposed, and it can be operated under multiple failure models. This method can integrate the multisensor monitoring data with the dynamic working condition data into the fusion data. Through the usage of bidirectional neural network in the deep learning, the time correlation model of the fusion data can be obtained. Then, this method can achieve nonlinear regression analysis of the fusion data and product remaining life under multiple failure models. This paper takes the remaining life prediction of wind turbine drive system as a case to prove the effectiveness of the method.

2. The Construction of Internet of Things (IoT) in the Drive System of Wind Turbine

The working environment of wind turbine drive system is hard, so it is necessary to monitor working conditions and environmental information. Therefore, a sensor is used to collect information as data support for the system. The sensor can convert physical signals into electrical signals so as to satisfy the actual demand [38]. Its accuracy affects the performance of the system, so the selection of sensors should take the system requirements and environment factors into consideration.

The state monitoring and life prediction system of the wind turbine drive system based on the Internet of Things can be divided into three functional levels. (a) Perception layer: The perception layer includes transmission equipment, sensors, and wireless sensor nodes. Its function is to perceive the working conditions of the transmission system. (b) Transmission layer: The transmission layer uses the CAN communication protocol to achieve wired communication between devices and uses the ZigBee communication protocol to build a wireless sensor network. Its function is to deliver the working condition information of the transmission system. (c) Application layer: The application layer is composed of PC/104, operating system, software, and life prediction algorithm. Its function is to achieve acceptance, storage, display, and intelligent processing of the working condition information and manage the entire life cycle of the wind turbine.

Figure 1 shows the system hardware framework. The wireless sensor network collects speed and temperature information of the transmission system and delivers them to the PC/104 for processing. At the same time, the ARM processor collects fault signals, status signals, current signals, and vibration signals of the transmission system and delivers them to the PC/104 for processing. The PC/104 processes the collected information and displays the results and status monitoring information on the LCD screen. The PC/104 can share the information with the centralized control center through the Ethernet communication module. Then, the centralized control center can monitor the transmission system in real time.

3. Data-Driven Fatigue Life Prediction Based on IoT

A large amount of data has been accumulated during the sensor operation. After being processed, the data still contain unused information. The data-driven multivariate statistical algorithm can use these data to carry out process monitoring, fault monitoring and diagnosis, and quality and life prediction [39–41].

The product remaining life is the time interval between the current moment and the failure moment. Specifically, the product monitoring information at this moment is compared with the historical information to get the comparison conclusion and predict the product remaining life.

3.1. Data Collection. The degradation status information of products during operation is monitored by multiple sensors. Then, the data is defined as online measurement data. The monitoring data of training products are recorded until failure and saved to $\{s^i, y^i\}_{i=1}^{L}$. $s^i \in \mathrm{R}^{M\times p}$ represents the online monitoring data of the i-th training product. The data are monitored by p sensors. Each sensor employs M data points. L is the total number of training products. y^i represents the degradation state of the i-th training product and needs to be detected offline. The monitoring data of texting products are recorded and saved to $\{s^j\}_{j=1}^{C}$. $s^j \in \mathrm{R}^{M\times p}$

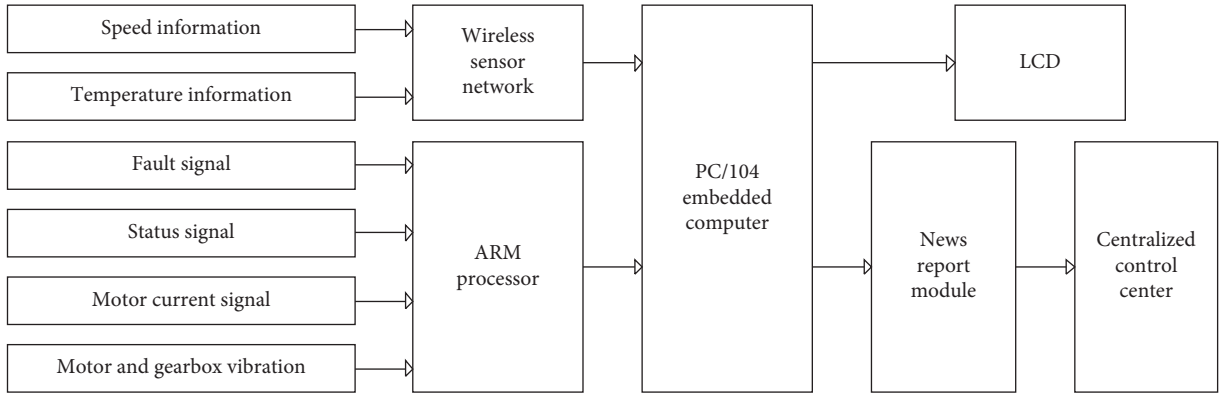

Figure 1: The frame diagram of system hardware.

represents the online real-time monitoring data of the j-th testing product. C is the total number of testing products. The information about the degradation status and remaining life of the testing product is unknown, and it needs to be further estimated based on $\{s^j\}_{j=1}^{C}$.

3.2. Data Preprocessing. The data preprocessing can be divided into three sections, namely, feature extraction, data regularization processing, and sliding time window processing.

The feature extraction of the monitoring data can reduce the data size and increase work efficiency. The noisy and abnormal data points will affect prediction accuracy of the method. The feature extraction can reduce the above-mentioned adverse effects. First, the time domain features of the monitoring data can be extracted, such as mean, standard deviation, root mean square, skewness, and kurtosis. Second, the frequency domain features of the monitoring data can be extracted by the fast Fourier transform technique, such as average frequency, spectral skewness, spectral kurtosis, and spectral power. Third, the time-frequency domain features can be extracted by the empirical mode decomposition and wavelet change technique.

After the above steps, the monitoring data $\{s^i\}_{i=1}^{L}$ and $\{s^j\}_{j=1}^{C}$ can be converted into set $\{x^i\}_{i=1}^{L}$ and $\{x^j\}_{j=1}^{C}$. $x^i \in \mathrm{R}^{1\times N}$ and $x^j \in \mathrm{R}^{1\times N}$ represent the initial features of the i-th training product s^i and the j-th testing product s^j. N represents the number of initial features. However, the extracted features have different data size, so the z-score regularization method is used to normalize data, as follows:

$$\widetilde{x}_d^k = \frac{x_d^k - \mu_d}{\sigma_d}, \tag{1}$$

where x_d^k represents the d-th feature quantity for the k-th sample, $\widetilde{x}_d^k$ represents the result after normalization, and μ_d and σ_d represent the mean and standard deviation of the d-th feature in set.

3.3. Life Prediction Method Based on Particle Filter Algorithm. The network structure based on the bidirectional long short-term memory (Bi-LSTM) model can be divided into two sections: (1) extracting the time-dependent features of normalized data by the Bi-LSTM network; (2) processing the time-dependent features and outputting the prediction result of product degradation indicators. A schematic diagram of the correlation between the two sections is shown in Figure 2.

More details can be found as follows:

Step 1: the training set $\{X^k, y^k\}_{k=1}^{K}$ can be obtained by processing monitoring data. $X^k = [x_1^k, x_2^k, \ldots, x_t^k, \ldots, x_{t_{\mathrm{TW}}}^k]$ represents the data of the k-th training feature. t_{TW} represents the length of the data. $x_t^k \in \mathrm{R}^{1\times N}$ represents the normalized feature data at time t. y^k represents the product degradation state of X^k. The value of y^k is the data of the offline degradation state. X^k is normalized and its time-dependent features are extracted by the Bi-LSTM network, as follows:

$$\left[h_1, h_2, \ldots, h_t, \ldots, h_{t_{\mathrm{TW}}}\right] = f_1\left(X^k, \overrightarrow{\Theta}_{BI-LSTM}, \overleftarrow{\Theta}_{\mathrm{BI}-LSTM}\right), \tag{2}$$

where f_1 represents the hidden layer function of the Bi-LSTM network. The parameter set of the Bi-LSTM network is described by $(\overrightarrow{\Theta}_{\mathrm{BI}-LSTM}, \overleftarrow{\Theta}_{\mathrm{BI}-LSTM})$.

All output features of the Bi-LSTM network are given in (2). However, only the output features of the last time point of the second layer are used for the fully connected layer; the calculation process is as follows:

$$h_{t_{\mathrm{TW}}} = \overrightarrow{h}_{t_{\mathrm{TW}}} \oplus \overleftarrow{h}_{t_{\mathrm{TW}}}, \tag{3}$$

where $\overrightarrow{h}_{t_{\mathrm{TW}}}$ and $\overleftarrow{h}_{t_{\mathrm{TW}}}$ represent the output features of the forward and reverse Bi-LSTM networks at the last moment, and $\oplus$ represents the sum operation point-by-point.

Step 2: The output feature $h_{t_{\mathrm{TW}}}$ of the Bi-LSTM network is used in the fully connected layer to further extract the advanced features. The calculation process is as follows:

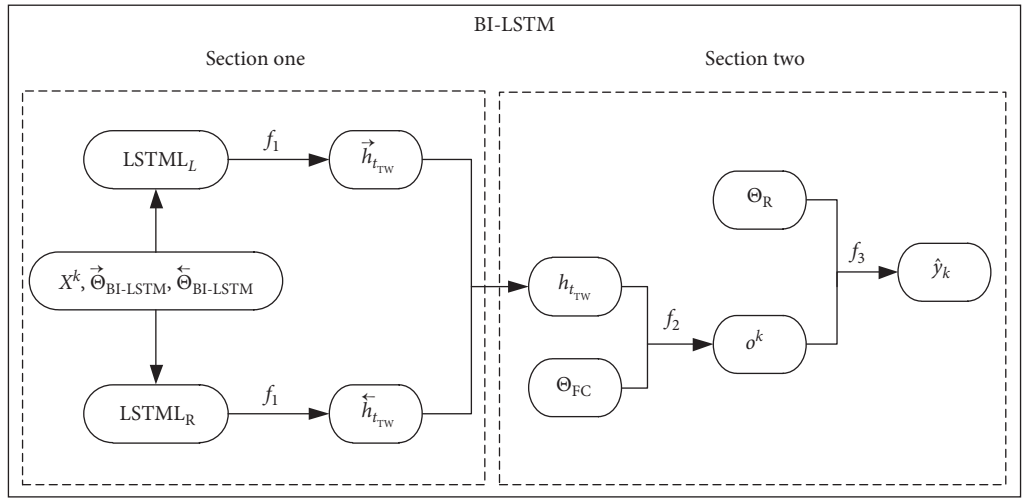

Figure 2: The diagram of the correlation between the two sections.

$$o^k = f_2\left(h_{t_{TW}}; \Theta_{FC}\right) = W_F h_{t_{TW}} + b_F, \tag{4}$$

where o^k is the output features of the fully connected layer and Θ_{FC} is the parameter set of the fully connected layer, including the weight matrix W_F and the bias vector b_F. Then, o^k is used to predict the degradation state of the product. The process can be described by the following equation:

$$\hat{y}_k = f_3\left(o^k; \Theta_R\right) = W_R o^k, \tag{5}$$

where $\hat{y}_k$ is the prediction of the product degradation index and W_R is the weight vector of the last linear regression layer.

Step 1 and Step 2 both use single-layer bidirectional long short-term memory neural network expression and fully connected neural network expression. In actual engineering, more layers can be stacked to form a deep structure. However, the deep neural network structure has a more complex model and needs more training data.

The calculation process of the model forward propagation has been given earlier. Then, the model loss function based on mean variance can be defined as follows:

$$L(\Theta) = \frac{1}{K}\sum_{k=1}^{K}\left(y^k - f_\Theta\left(X^k\right)\right)^2, \tag{6}$$

where y^k represents the normalized value of the degradation indicators in the shutdown state, $y^k = f_\Theta(X^k)$ represents the prediction of the product degradation indicators X^k, and $f_\Theta(\bullet)$ is defined by (2)–(5).

For some complex products, the degradation state data is difficult to obtain online directly because of actual engineering limitations. Hence, online monitoring techniques are used as auxiliary means to obtain indirect data and complete the estimation of the degradation state. In order to define the problem of product degradation state estimation, firstly, the relationship between the degradation state and time is given as follows:

$$y_k = f\left(y_{k-1}, v_{k-1}\right) \Longleftrightarrow p\left(y_k \mid y_{k-1}\right), \tag{7}$$

where k represents the time point, $f(\bullet)$ represents the product state transition model, y_{k-1} represents the internal degradation state of the product at time k-1, and v_{k-1} represents an independent and identically distributed process noise. At any time point k, the online measurement data $s_k \in \mathrm{R}^{M\times p}$ of the product can be obtained, and the nonlinear relationship between s_k and y_k is given as follows:

$$s_k = h\left(y_k, w_k\right) \Longleftrightarrow p\left(s_k \mid y_k\right), \tag{8}$$

where $h(\cdot)$ is the observation model and w_k is an independent and identically distributed measurement noise.

The online measurement data is collected by multiple sensors at very high sampling frequency, and its signal to noise ratio is low, so it is difficult to obtain the display analytical model between the online monitoring data and the internal degradation state. Therefore, the online measurement data is processed earlier, including feature extraction, normalization, and serialization. Then, the online monitoring data can be converted into a set of normalized data $x_k = [x_1^k, x_2^k, \ldots, x_t^k, \ldots, x_{t_{TW}}^k] = f_{\text{Pre-processing}}(s_k)$. Finally, the model between the extracted feature x_k and the internal degradation state y_k is established based on the Bi-LSTM network and is given as follows:

$$z_k = h_{\text{BI-LSTM}}\left(y_k, x_k, w_k\right) \Longleftrightarrow p\left(z_k \mid y_k\right), \tag{9}$$

where z_k represents the predicted output value of the product degradation index, y_k represents the internal degradation state of the product in the shutdown state, and w_k is the measurement noise and follows a normal distribution.

In the framework of Bayesian learning, the main task is to calculate the posterior probability distribution $p(y_{k+1} \mid s_{k+1})$ of the product degradation state when the real-time online measurement data s_{k+1} is known [42–47]. s_{k+1} is processed and transmitted to the Bi-LSTM network to obtain the product degradation index predicted output value

z_{k+1}. Thus, the posterior probability distribution $p(y_{k+1} \mid z_{k+1})$ is actually obtained. If $p(y_k \mid z_k)$ is known at time k, the probability density function $p(y_{k+1} \mid z_k)$ based on the Chapman–Kolmogorov equation is given as follows:

$$p\left(y_{k+1} \mid z_k\right) = \int p\left(y_{k+1} \mid y_k\right)\left(y_k \mid z_k\right)\mathrm{d}y_k. \tag{10}$$

At time $k+1$, the new online measurement data s_{k+1} is processed and transmitted to the Bi-LSTM network to obtain the product degradation index prediction output z_{k+1}. Then, the posterior probability distribution $p(y_{k+1} \mid z_{k+1})$ can be updated based on the Bayesian criterion as follows:

$$p\left(y_{k+1} \mid z_{k+1}\right) = \frac{p\left(z_{k+1} \mid y_{k+1}\right)p\left(y_{k+1} \mid z_k\right)}{p\left(z_{k+1} \mid z_k\right)}, \tag{11}$$

where $p(z_{k+1} \mid y_{k+1})$ represents the likelihood function at time $k+1$ and can be defined by (9), the probability density distribution $p(y_{k+1} \mid z_k)$ can be calculated through the prediction, and $p(z_{k+1} \mid z_k)$ represents the normalization factor. The calculation process is as follows:

$$p\left(z_{k+1} \mid z_k\right) = \int p\left(z_{k+1} \mid y_{k+1}\right)\left(y_{k+1} \mid z_k\right)\mathrm{d}y_{k+1}. \tag{12}$$

Because of the nonlinear features, it is difficult to obtain exact solutions of above equations, so particle filtering is introduced to solve these problems. The structure of particle filtering is actually the Monte Carlo method (which refers to the probability of the event by the frequency of occurrence at a certain time) with a layer of importance sampling proposed in it. The basic idea of this method is to use a set of samples (or particles) to approximate the posterior probability distribution of the system, and then use this approximate representation to estimate the state of the nonlinear system. Using this idea, particle filtering can handle any form of probability in the filtering process. At the same time, $p(y_{k+1} \mid z_{k+1})$ is approximated by Bayesian filtering method based on Monte Carlo simulation. If $p(y_k \mid z_k)$ is known at time k and can be described by discrete values $y_k^1, \ldots, y_k^i, \ldots, y_k^N$ and their weights $\omega_k^1, \ldots, \omega_k^i, \ldots, \omega_k^N$, the calculation process is given as follows:

$$p\left(y_k \mid z_k\right) \approx \sum_{i=1}^{N} \omega_k^i \delta\left(y_k - y_k^i\right), \tag{13}$$

where $\sum_{i=1}^{N} \omega_k^i = 1$, $\delta(\cdot)$ represents the Dirac δ function.

Equation (10) can be rewritten as follows:

$$\begin{aligned} p\left(y_{k+1} \mid z_k\right) &\approx \sum_{i=1}^{N} \omega_k^i \delta\left(y_k - y_k^i\right) p\left(y_{k+1} \mid y_k\right) \\ &= \sum_{i=1}^{N} \omega_k^i p\left(y_{k+1} \mid y_k\right), \end{aligned} \tag{14}$$

where i represents the i-th particle, N represents the total number of particles, and $p(y_{k+1} \mid y_k)$ can be calculated based on the state transition model.

The weight value ω_k^i of (9) can be updated by the importance sampling method, and the update process is given as follows:

$$\omega_{k+1}^i \propto \omega_k^i p\left(z_{k+1} \mid y_k^i\right), \tag{15}$$

where $p(z_{k+1} \mid y_k^i)$ represents the likelihood function of the predicted output z_{k+1}.

In order to avoid the particle degradation during the operation of the particle filtering algorithm, the resampling method based on the inverse cumulative function is used to obtain particles with equal weights. The steps are as follows: Step 1. Construct the cumulative density function based on the likelihood function $p(z_{k+1} \mid y_k^i)$. Step 2. Sample a random value from the uniform distribution U (0, 1) and use it as the input of the cumulative density function in Step 1. Step 3. Take out the particle whose value is most similar to the output of CDF in Step 2 and consider it as the result after resampling. Step 4. Repeat the calculation process of Steps 1–3 N times and obtain N equal weight resampling particles. Then, use these particles to approximate the posterior probability density distribution $p(y_{k+1} \mid z_{k+1})$.

4. Case Study

4.1. Doubly Fed Wind Turbine Drive System. The wind turbine drive system can transmit torque and change rotating speed. Its structure has a great influence on the layout of wind turbine. At present, the wind turbine has two types: doubly fed and direct-drive. The difference between them is the structure of the drive system. The drive system of the doubly fed wind turbine has a speed-increasing gearbox, while the drive system of the direct-drive wind turbine does not have one. The object of this paper is the doubly fed wind turbine drive system.

The wheel hub of the doubly fed wind turbine is connected to one side of the low-speed main shaft. The other side is connected to the input of the speed-increasing gearbox. The output of the gearbox (high-speed shaft) is connected to the generator rotor through the flexible coupling. The hydraulic brake disc is installed on the high-speed shaft. The entire drive system is installed on the main frame. The thrust and radial load generated by the wind wheel are transmitted to the main frame first and then to the tower.

Because of the speed-increasing gearbox, the generator rotor can reach a high rotating speed and the requirement for magnetic poles is low. The gearbox calls for a high speed-increasing ratio and use multistage planetary gears combined with fixed-shaft gears. The characteristics of the doubly fed wind turbine drive system are as follows: (1) The operating conditions change with the wind speed and lead to constant change of vibration signal amplitude and frequency. As a result, the signal contains a large number of uncertainties. (2) The drive system is located in the top of the tower. Strong wind will cause the body shake. Hence, the signal will contain noise interference. (3) The mechanical structure of wind turbine drive system is complex. It calls for high standard of related technologies. (4) Wind turbines are

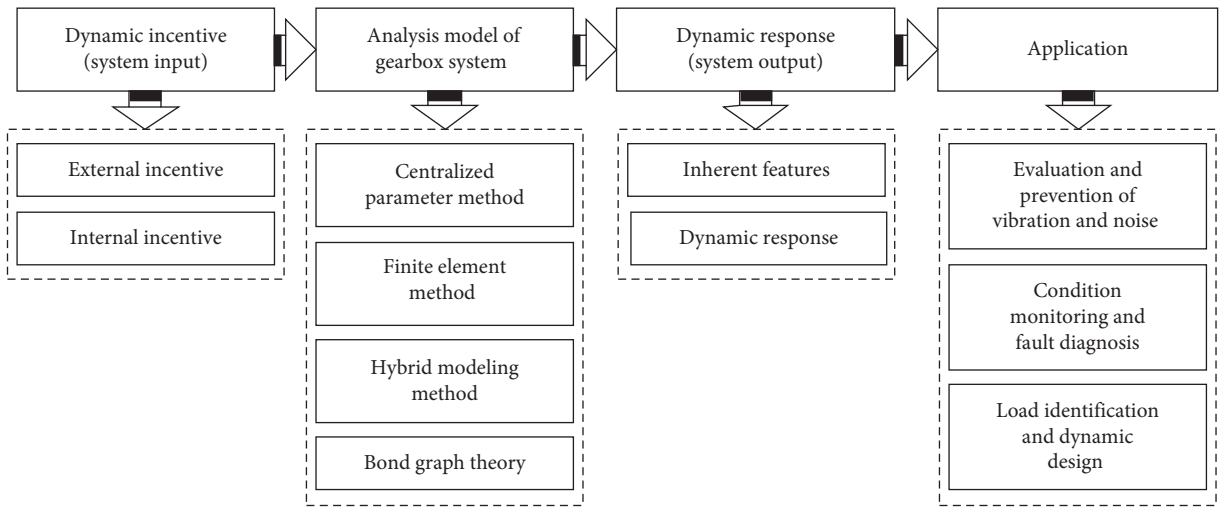

Figure 3: Dynamic modeling and analysis process of wind turbine gearbox.

severely affected by environmental conditions and have high requirements for the reliability and anti-interference ability of the test system.

4.2. Dynamic Modeling of Wind Turbine Drive System. This paper uses the dynamic analysis process of the wind turbine gearbox drive system as shown in Figure 3.

First of all, the external and internal incentives of the gearbox are obtained through the monitoring of the Internet of Things technology. They are transmitted as dynamic incentives to the analysis model of gearbox system. Second, the analysis model of gearbox system processes the input dynamic incentives through centralized parameter method, finite element method, hybrid modeling method, and bong graph theory. After processing, the inherent features and dynamic responses are output, and they are used as the dynamic responses of the analysis system. Finally, the particle filter algorithm is used for condition monitoring and life prediction applications. The above is the main application process of the method proposed in this paper for the wind turbine drive system.

The external excitation of the gearbox mainly includes the dynamic input torque, the nontorsional loads, the generator feedback torque, the braking torque, and the impact load. The internal excitation includes time-varying stiffness excitation, time-varying error excitation, meshing shocks, and tooth backlash. This paper uses dynamic response analysis method, dynamic stability analysis method, and inherent characteristic analysis method to optimize the system structure. Based on the IoT technology, the dynamic model has been proposed to monitor the gearbox status and provide theoretical basis of fault diagnosis and life prediction.

4.3. Method Validation. The gearbox wear tests are recorded as A1, A2, and A3. Each test includes online monitoring data from six signal channels, and each test collected 600 sets of online monitoring data during transmission process. In order to describe the online monitoring data clearly, 50 equidistant data monitoring points are used for each online monitoring data group.

Table 1: Influence of feature selection steps on prediction results.

Optimal feature set	20	15	13	10	5
Root mean square error	7.14	5.78	5.24	5.09	4.97
Mean absolute error	6.89	5.68	5.87	5.02	4.75

Table 2: Influence of feature selection steps on prediction results.

Number of principal components retained (%)	95	97	99
Root mean square error	3.17	4.23	5.24
Mean absolute error	3.07	3.48	4.35

In order to reduce the data size and improve prediction efficiency, the method extracts the time domain feature first and then the frequency domain feature. The BL-STM model has been used to simplify the feature processing flow.

During the experiment, A1 is used as the test sample, and A2 and A3 are used as the training samples. The prediction result of the final transmission pair loss is shown in Table 1. According to the experiment results, the top five features with the highest scores can achieve the best prediction performance.

The influence of the feature fusion step on the final transmission pair loss prediction result is shown in Table 2. The optimal feature set used in Table 2 is composed of the top eight features with the highest scores. It can be inferred from Table 2 that the fusion feature with the highest scores can bring the best prediction performance.

Combined with the state transfer model of transmission pair wear and its observation model based on Bi-LSTM, the particle filter algorithm is used to predict the evolution of the transmission pair degradation index. When the index exceeds the failure threshold, the remaining useful life (RUL) of transmission pair can be obtained.

5. Conclusions

Based on the bidirectional long short-term memory neural network and particle filter technology, the remaining life prediction method for wind turbine drive system is proposed. Compared with the traditional method, it simplifies the feature processing flow by using deep learning technology. Through the engineering examples, the effectiveness of the method proposed in this paper has been proved. The research results in this paper will further promote the engineering application of deep learning technology to the product fatigue life prediction higher safety requirements.

Data Availability

All data used to support the findings of this study are included within the article.

Conflicts of Interest

The authors declare that they have no conflicts of interest regarding the publication of this paper.

Acknowledgments

This research was supported by the National Key Research Development Plan Funds under contract no. 2018YFB1702804.

References

[1] D. Meng, Z. Hu, P. Wu, S.-P. Zhu, J. A. F. O. Correia, and A. M. P. De Jesus, "Reliability-based optimisation for offshore structures using saddlepoint approximation," *Proceedings of the Institution of Civil Engineers—Maritime Engineering*, vol. 173, no. 2, pp. 33–42, 2020.

[2] D. Meng, Y. Li, S.-P. Zhu, Z. Hu, T. Xie, and Z. Fan, "Collaborative maritime design using sequential optimisation and reliability assessment," *Proceedings of the Institution of Civil Engineers—Maritime Engineering*, vol. 173, no. 1, pp. 3–12, 2020.

[3] R. Yuan, H. Li, and Q. Wang, "An enhanced genetic algorithm-based multi-objective design optimization strategy," *Advances in Mechanical Engineering*, vol. 10, no. 7, pp. 1–6, 2018.

[4] R. Yuan, H. Li, Z. Gong et al., "An enhanced Monte Carlo simulation-based design and optimization method and its application in the speed reducer design," *Advances in Mechanical Engineering*, vol. 9, no. 9, pp. 1–7, 2017.

[5] R. Yuan and H. Li, "A multidisciplinary coupling relationship coordination algorithm using the hierarchical control methods of complex systems and its application in multidisciplinary design optimization," *Advances in Mechanical Engineering*, vol. 9, no. 1, pp. 1–11, 2017.

[6] D. Meng, Y. Li, S.-P. Zhu, G. Lv, J. Correia, and A. De Jesus, "An enhanced reliability index method and its application in reliability-based collaborative design and optimization," *Mathematical Problems in Engineering*, vol. 2019, Article ID 4536906, 10 pages, 2019.

[7] B. Liu and Y. Deng, "Risk evaluation in failure mode and effects analysis based on D numbers theory," *International Journal of Computers, Communications & Control*, vol. 14, no. 5, pp. 672–691, 2019.

[8] H. Wang, Y. P. Fang, and E. Zio, "Risk assessment of an electrical power system considering the influence of traffic congestion on a hypothetical scenario of electrified transportation system in New York state," *IEEE Transactions on Intelligent Transportation Systems*, pp. 1–14, 2019.

[9] L. Pan and Y. Deng, "Probability transform based on the ordered weighted averaging and entropy difference," *International Journal of Computers Communications & Control*, vol. 15, no. 4, p. 3743, 2020.

[10] C. Sun, S. Li, and Y. Deng, "Determining weights in multi-criteria decision making based on negation of probability distribution under uncertain environment," *Mathematics*, vol. 8, no. 2, p. 191, 2020.

[11] R. Liu, P. Chen, X. Zhang, and S. Zhu, "Non-shock ignition probability of octahydro-1,3,5,7-tetranitro-tetrazocine-based polymer bonded explosives based on microcrack stochastic distribution," *Propellants, Explosives, Pyrotechnics*, vol. 45, no. 4, pp. 568–580, 2020.

[12] D. Liao, S.-P. Zhu, B. Keshtegar, G. Qian, and Q. Wang, "Probabilistic framework for fatigue life assessment of notched components under size effects," *International Journal of Mechanical Sciences*, vol. 181, Article ID 105685, 2020.

[13] S.-P. Zhu, B. Keshtegar, S. Chakraborty, and N.-T. Trung, "Novel probabilistic model for searching most probable point in structural reliability analysis," *Computer Methods in Applied Mechanics and Engineering*, vol. 366, Article ID 113027, 2020.

[14] X. Liang, M. J. Zuo, and M. Pandey, "Analytically evaluating the influence of crack on the mesh stiffness of a planetary gear set," *Mechanism and Machine Theory*, vol. 76, pp. 20–38, 2014.

[15] S. Li and A. Kahraman, "A micro-pitting model for spur gear contacts," *International Journal of Fatigue*, vol. 59, pp. 224–233, 2014.

[16] R. Yuan, H. Li, and Q. Wang, "Simulation-based design and optimization and fatigue characteristics for high-speed backplane connector," *Advances in Mechanical Engineering*, vol. 11, no. 6, pp. 1–10, 2019.

[17] H. Dong, C. Zhang, X. Wang, and D. Wang, "A precise FE model of a spur gear set considering eccentric error for quasi-static analysis," in *Mechanism and Machine Science*, pp. 1263–1274, Springer, Singapore, 2017.

[18] G. Dong, M. Jing, and H. Liu, "The study of elastohydrodynamic lubrication for the dynamic analysis of rolling bearing," in *Proceedings of the 2013 IEEE International Symposium on Assembly and Manufacturing (ISAM)*, pp. 297–299, Xi'an, China, July 2013.

[19] A. Leblanc, D. Nelias, and C. Defaye, "Nonlinear dynamic analysis of cylindrical roller bearing with flexible rings," *Journal of Sound & Vibration*, vol. 325, no. 1-2, pp. 145–160, 2009.

[20] L. Cui and Z. Qian, "Study on dynamic properties of roller bearing with nonlinear vibration," in *Proceedings of the 2010 International Conference on Mechanic Automation and Control Engineering*, pp. 2723–2726, Wuhan, China, June 2010.

[21] O. D. Mohammed, M. Rantatalo, and J.-O. Aidanpää, "Dynamic modelling of a one-stage spur gear system and vibration-based tooth crack detection analysis," *Mechanical Systems and Signal Processing*, vol. 54-55, pp. 293–305, 2015.

[22] X. Li, Y. Zhu, Z. Zhou, and N. Wang, "Fault diagnosis based on nonlinear dynamic modeling in rolling element bearing systems," in *Proceedings of the 2013 IEEE International*

Symposium on Assembly and Manufacturing (ISAM), pp. 12–15, Xi'an, China, July 2013.

[23] J. Liu, Z. Shi, and Y. Shao, "An analytical model to predict vibrations of a cylindrical roller bearing with a localized surface defect," *Nonlinear Dynamics*, vol. 89, no. 3, pp. 2085–2102, 2017.

[24] A. Rafsanjani, S. Abbasion, A. Farshidianfar, and H. Moeenfard, "Nonlinear dynamic modeling of surface defects in rolling element bearing systems," *Journal of Sound and Vibration*, vol. 319, no. 3–5, pp. 1150–1174, 2009.

[25] L. Niu, H. Cao, H. Hou, B. Wu, Y. Lan, and X. Xiong, "Experimental observations and dynamic modeling of vibration characteristics of a cylindrical roller bearing with roller defects," *Mechanical Systems and Signal Processing*, vol. 138, Article ID 106553, 2020.

[26] Y. Cui, S. Deng, W. Zhang, and G. Chen, "The impact of roller dynamic unbalance of high-speed cylindrical roller bearing on the cage nonlinear dynamic characteristics," *Mechanism and Machine Theory*, vol. 118, pp. 65–83, 2017.

[27] S. E. Deng, J. H. Fu, Y. S. Wang, and H. S. Yang, "Analysis on dynamic characteristics of aero-engine rolling bearing/dual-rotor system," *Journal of Aerospace Power*, vol. 28, no. 1, pp. 195–204, 2013.

[28] L. Xiang, Y. Zhang, N. Gao, A. Hu, and J. Xing, "Nonlinear dynamics of a multistage gear transmission system with multi-clearance," *International Journal of Bifurcation and Chaos*, vol. 28, no. 3, Article ID 1850034, 2018.

[29] X. Liang, M. J. Zuo, and Z. Feng, "Dynamic modeling of gearbox faults: a review," *Mechanical Systems and Signal Processing*, vol. 98, pp. 852–876, 2018.

[30] M. A. Ghaffari, Y. Zhang, and S. Xiao, "Multiscale modeling and simulation of rolling contact fatigue," *International Journal of Fatigue*, vol. 108, pp. 9–17, 2018.

[31] J. D. Martínez-Morales, E. R. Palacios-Hernández, and D. U. Campos-Delgado, "Multiple-fault diagnosis in induction motors through support vector machine classification at variable operating conditions," *Electrical Engineering*, vol. 100, no. 1, pp. 59–73, 2018.

[32] P. Boškoski and Đ. Juričić, "Fault detection of mechanical drives under variable operating conditions based on wavelet packet Rényi entropy signatures," *Mechanical Systems & Signal Processing*, vol. 31, pp. 369–381, 2012.

[33] H. Vold and J. Leuridan, "High resolution order tracking at extreme slew rates, using Kalman tracking filters," *Shock & Vibration*, vol. 2, no. 6, pp. 507–515, 1995.

[34] D. Meng, S. Yang, Y. Zhang, and S. P. Zhu, "Structural reliability analysis and uncertainties-based collaborative design and optimization of turbine blades using surrogate model," *Fatigue & Fracture of Engineering Materials & Structures*, vol. 42, no. 6, pp. 1219–1227, 2019.

[35] S.-P. Zhu, Z.-Y. Yu, Q. Liu, and A. Ince, "Strain energy-based multiaxial fatigue life prediction under normal/shear stress interaction," *International Journal of Damage Mechanics*, vol. 28, no. 5, pp. 708–739, 2019.

[36] D. Meng, T. Xie, P. Wu et al., "Uncertainty-based design and optimization using first order saddlepoint approximation method for multidisciplinary engineering systems," *ASCE-ASME Journal of Risk and Uncertainty in Engineering Systems, Part A: Civil Engineering*, vol. 6, no. 3, Article ID 04020028, 2020.

[37] D. Meng, Y. F. Li, H. Z. Huang, Z. Wang, and Y. Liu, "Reliability-based multidisciplinary design optimization using subset simulation analysis and its application in the hydraulic transmission mechanism design," *Journal of Mechanical Design*, vol. 137, no. 5, Article ID 051402, 2015.

[38] C. Dürager, A. Heinzelmann, and D. Riederer, "A wireless sensor system for structural health monitoring with guided ultrasonic waves and piezoelectric transducers," *Structure and Infrastructure Engineering*, vol. 9, no. 11, pp. 1177–1186, 2013.

[39] S. P. Zhu, Q. Liu, Q. Lei, and Q. Wang, "Probabilistic fatigue life prediction and reliability assessment of a high pressure turbine disc considering load variations," *International Journal of Damage Mechanics*, vol. 27, no. 10, pp. 1569–1588, 2018.

[40] S.-P. Zhu, Q. Liu, W. Peng, and X.-C. Zhang, "Computational-experimental approaches for fatigue reliability assessment of turbine bladed disks," *International Journal of Mechanical Sciences*, vol. 142-143, pp. 502–517, 2018.

[41] S. P. Zhu, Q. Liu, J. Zhou, and Z. Y. Yu, "Fatigue reliability assessment of turbine discs under multi-source uncertainties," *Fatigue & Fracture of Engineering Materials & Structures*, vol. 41, no. 6, pp. 1291–1305, 2018.

[42] J. Dai and Y. Deng, "A new method to predict the interference effect in quantum-like Bayesian networks," *Soft Computing*, vol. 24, no. 14, pp. 10287–10294, 2020.

[43] Q. Cai and Y. Deng, "A fast Bayesian iterative rule in amoeba algorithm," *International Journal of Unconventional Computing*, vol. 5, no. 19, pp. 449–466, 2019.

[44] S.-P. Zhu, H.-Z. Huang, W. Peng, H.-K. Wang, and S. Mahadevan, "Probabilistic Physics of Failure-based framework for fatigue life prediction of aircraft gas turbine discs under uncertainty," *Reliability Engineering & System Safety*, vol. 146, pp. 1–12, 2016.

[45] S.-P. Zhu, H.-Z. Huang, R. Smith, V. Ontiveros, L.-P. He, and M. Modarres, "Bayesian framework for probabilistic low cycle fatigue life prediction and uncertainty modeling of aircraft turbine disk alloys," *Probabilistic Engineering Mechanics*, vol. 34, pp. 114–122, 2013.

[46] R. Yuan, M. Tang, H. Wang, and H. Li, "A reliability analysis method of accelerated performance degradation based on bayesian strategy," *IEEE Access*, vol. 7, pp. 169047–169054, 2019.

[47] H. Li, R. Yuan, and J. Fu, "A reliability modeling for multi-component systems considering random shocks and multi-state degradation," *IEEE Access*, vol. 7, pp. 168805–168814, 2019.